

# **A rapid and non-destructive discrimination and source correspondence of tyres by Raman spectroscopy combined with chemometrics**

## **Abstract**

Identifying and comparing the tyre (rubber) threads are crucial in forensic investigations involving collision accidents and hit-and-run incidents. Focusing on improving the effectiveness of tyre classification and identification, the current study pioneered the utilisation of Raman spectroscopy combined with PLS-DA on 140 samples of light-motor vehicle (LMV) and heavy-motor vehicle (HMV) automobile tyres. All the spectral peaks were examined from the region of 400–2000  $\text{cm}^{-1}$ , which indicated the molecular vibrations of tyre (rubber) composition. Meanwhile, the chemometric method of PLS-DA achieved a very highly accurate (99.4%) classification between LMV and HMV samples. The model was further tested using 17 unknown samples (treated as blind samples). 94.1% of these blind samples were accurately predicted into their respective classes. Following after 6 months period, the study proceeded to explore the application of the PLS-DA model in real settings using 12 different unknown samples after scratch on the road, which resulted in 83.3% correct predictions. To the best of our knowledge, this study is the most comprehensive study in tyre classifications and source correspondence as a non-destructive approach to examine tyre rubber, yielding valuable insights for related crime scene investigations.

**Keywords:** Chemometrics; rubber; Raman spectroscopy; partial least square discriminant analysis

## 1. Introduction

The resulting path that each tyre yields when a vehicle moves in any direction is part of the track evidence. In a crime scene investigation, track evidence after vehicle crash is valuable evidence for including or excluding the suspect vehicles [1,2]. Taking the case of under-running or tailgating, a sudden and unexpected halt of a heavy vehicle may cause another vehicle to drive into the back of that heavy vehicle. The friction force between the tyres and the road after the brake application yields rubber traces as evidentiary material. In circumstances of indistinguishable tyre treads, rubber traces transferred from the tyres to the road may indicate the tyre identity by comparing the remnants of rubbers (the questioned samples) with the rubber material from the suspect vehicle tyres (control samples) [1,2].

A tyre has several key constituents, such as rubber (isoprene or natural rubber, 1, 3-butadiene [BR], and styrene-butadiene copolymer [SBR]), fillers (carbon black and silica), extender oils (distilled aromatic extract oils), vulcanising agents (sulphur), accelerators (benzothiazoles), activators (zinc oxide and stearic acid), processing aids (peptizers, plasticizers, and softeners), and protective agents (antioxidants and antiozonants) [3]. There are various advanced methods available to analyse the chemical composition of tyre (rubber), such as chromatographic analysis [4,5], simultaneous thermal analysis (STA) [6], micro-X-ray fluorescence spectroscopy (XRF) [6], and laser-induced breakdown spectrometry (LIBS) [7]. The vibrational ATR-FTIR techniques have increasingly been preferred in recent forensic investigations due to their non-destructive nature. Numerous studies have used non-destructive techniques of ATR-FTIR in various fields, such as soil [8], kohl [9], hair [10], cigarette filter [11], and blood stain [12].

For instance, focusing on the application of ATR-FTIR and chemometrics, He et al. [13] performed principal component analysis (PCA) and discriminant analysis (DA) on 240 tyres of different brands in China to develop a predictive classification model. The results of DA revealed perfect differentiation between brand groupings and sample classifications, but the spectral comparison showed no meaningful separation via PCA. After three years from He et al.'s [13] study, Haojun Du et al. [14] applied ATR-FTIR combined with machine learning algorithms, specifically logistic regression (LR), random forest (RF), weighted k-nearest neighbour analysis (WKNN), and support vector machine (SVM), to discriminate 187 tyres found in China. SVM recorded the highest recognition rate (100%), whereas RF recorded the lowest recognition rate (88.4%). The prediction models in both of these studies [13,14] did not use unknown or blind samples (useful in forensic case scenario). In a more recent study, Kaur et al. [21] applied machine learning methods of extra tree classifier (ET), LR, and RF to discriminate brands of two tyre classes (HMV and LMV). The study noted ATR-FTIR spectrometer equipped with diamond crystal in previous studies conducted by He et al. [13] and Haojun Du et al. [14] produced better outcomes than ATR instrument with a Ge crystal, as the latter possesses higher sensitivity on the damage caused by abrasive sample components. The study further noted a higher classification rate of ET (90%), as compared to other machine learning and examined the use of external samples in assessing the prediction scores of classifiers.

There have been other recent studies on the application of chemometrics on ATR-FTIR data to classify and discriminate tyres [13,14]. Kaur et al. [21] used machine learning to class the HMV and LMV samples using ATR-FTIR spectroscopy. However, brand discrimination was not analysed in this study and the real forensic cases was fully reported in the study. The current

study pioneered the application of Raman spectroscopy combined with chemometrics to analyse brand classifications and traces of tyres obtained from the road, yielding results that may be applicable to more complex situations. This study demonstrated how to reduce the number of manufacturers according to the brands, which can help forensic investigators to narrow down the search of suspects involved in vehicle collisions based on the deposited rubber traces on the road.

Thus, the current study employed alternative vibrational and non-destructive method of Raman spectroscopy combined with chemometrics for the discrimination of two classes of tyres (HMV and LMV, each with 7 brands and each brand having 10 samples). This study has two parts; firstly, we performed partial least square discriminant analysis (PLS-DA) for supervised classification of the main types of HMV and LMV; secondly the different brands in each category were also classified. PLS-DA's capacity to reduce large correlated variables to a new subspace of small set of orthogonal variables called PLS components, allows the prediction of the Y variables [15]. This study explored the benefits of PLS-DA model, which would greatly benefit actual forensic cases that are generally more complex in nature. There may be scenarios involving tyre deposition and its timing during vehicle collision or clash, where rubber is smeared on the road in minute traces. The spectra of these traces can be projected to the already classified samples and can assign a class to the unknown smears. This methodology offers reliable and practical means in forensic investigations.

## **2. Materials and Methods**

### *2.1 Sample collection*

140 tyre samples were purchased from automobile dealers and automobile workshops in Malaysia. As shown in Table 1, seven tyre brands were gathered, and 10 samples of each brand

were acquired for each tyre type (HMV and LMV). All different brands were obtained in triplicate (three samples for each brand) to assess whether any intra-brand variations were present. Considering the focus of this study on the area in direct contact with the road, all samples were collected from the thread section of the tyre using gloves to reduce contamination risk. Table 1 indicate the details on date of manufacturer through Department of transportation (DOT) number. The date of manufacturing is indicated by the DOT number. The final two figures represent the year of fabrication, while the first two represent the week (Fig. S.1).

**Table 1. Tyre analysed in the study.**

<b>Samples</b>	<b>Brand Name/ Model</b>	<b>Size</b>	<b>Manufacturer</b>	<b>DOT</b>	<b>Type</b>
A1-A10	Eudemon UF 195	355/80R16	China	3222	HMV
B1-B10	Carleo CA85	325/80R17	China	0921	HMV
C1-C10	Centara 185	315/80R18	China	2422	HMV
D1-D10	Michelin X Line Energy Z	325/80R22	France	0821	HMV
E1-E10	Bridgestone M726	315/70R19	Japan	1221	HMV
F1-F10	Continental HS3	325/70R22	Germany	0922	HMV
G1-G10	Cooper Roadmaster	305/75R24	USA	1123	HMV

	RM832 EM				
H1-H10	Hankook Kinergy Eco 2	135/50R12	South Korea	0824	LMV
I1-I10	Michelin Sport 4	135/55R15	France	2320	LMV
J1-J10	Good year Assurance Triple Max	115/55R16	USA	0819	LMV
K1-K10	Nexen N Fera	125/60R12	South Korea	0522	LMV
L1-L10	Dunlop SP	125/60R13	Malaysia	0621	LMV
M1-M10	Achilles ATR	135/60R13	Indonesia	0522	LMV
N1-N10	Viking Tech GT6	125/60R14	Germany	3523	LMV

## 2.2 Raman spectral analysis

Tyre samples were analysed using Raman spectrometer (Foram 685, Foster + Freeman, United Kingdom) equipped with a thermoelectrically cooled (20°C), back-thinned, two-dimensional binning charge-coupled detector with ×20 magnification objective lens. Prior to the analysis, the spectrometer was pre-calibrated with silicon chip. FORAM software was utilised for the pre-processing of Raman spectrum (baseline corrected) to reduce possible noise from the sample. The optimal parameters were used at the resolution of 16 cm<sup>-1</sup> with four scans at the

range of 400–2000  $\text{cm}^{-1}$ . In addition, samples were evaluated three times from three different points to evaluate its repeatability, and Raman spectroscopy was assessed with three different samples of the same type to evaluate its reproducibility.

### 2.3 Chemometrics: PLS-DA

The spectral data were then classified and discriminated through PLS-DA using the mixOmics package in R software. The analysis transformed the original spectral data to latent variables of reduced dimensions, which served as the dimensions of the PLS-DA model [15]. The supervised nature of PLS-DA allowed the discrimination of the samples and sample classes through the sample plot in this study. As for the prediction, the best parameters of the model were determined based on the classification error rate, receiver operating characteristic (ROC) curve and area under the curve (AUC), balanced error rate (BER), and confusion matrix [15-18].

## 3. Results

### 3.1 Preliminary discrimination of Raman spectra

Referring to Fig. 1(a-b), the Raman peak profiles revealed similar shapes for both HMV and LMV. However, both tyre types exhibited notably different characteristics for Raman peaks ranging from 400 to 2000  $\text{cm}^{-1}$ . In the case of HMV, the observed peaks were around 535  $\text{cm}^{-1}$ , 680  $\text{cm}^{-1}$ , 1350  $\text{cm}^{-1}$ , 1420  $\text{cm}^{-1}$ , and 1550  $\text{cm}^{-1}$ . As for the case of LMV, the observed peaks were around 462  $\text{cm}^{-1}$ , 510  $\text{cm}^{-1}$ , 680  $\text{cm}^{-1}$ , 700  $\text{cm}^{-1}$ , 750  $\text{cm}^{-1}$ , 1150 $\text{cm}^{-1}$ , 1320 $\text{cm}^{-1}$ , 1360  $\text{cm}^{-1}$ , and 1520  $\text{cm}^{-1}$ . Based on the results in Table 2, the observed peak at 1150  $\text{cm}^{-1}$  was linked to the presence of S=O stretching, symmetrical C–H bond deformations in  $\text{Si}(\text{CH}_3)_2$ , and C = C–H (1, 2

addition) bending vibrations. Meanwhile, the observed peaks at  $700\text{ cm}^{-1}$  and  $750\text{ cm}^{-1}$  were associated with the presence of 1, 4-butadiene (BR), and styrene-butadiene copolymer (SBR). The observed peaks at  $462\text{ cm}^{-1}$  and  $535\text{ cm}^{-1}$  corresponded to the C-N-S bending vibrations. Fig. S.2 indicates intra-brand variations of J tyres and minor variability in spectral shape was observed between a set of three spectra. Further evaluation on relative standard deviation (%RSD) was  $<0.1\%$  indicates the precision of Raman analysis.

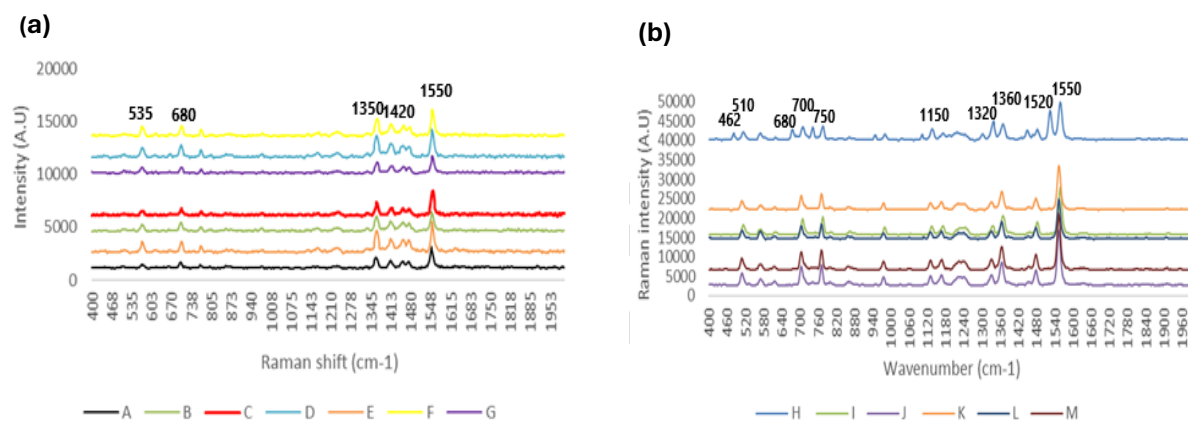


**Fig. 1: (a) Raman spectra of tyre samples of HMV and (b) Raman spectra of tyre samples of LMV.**

**Table 2: Raman peaks and their assignment (functional group) observed in tyre samples [22]**

Peak ( $\text{cm}^{-1}$ )	Assignments
462	C-N-S bending vibrations
535	C-N-S bending vibrations

680	C–H (benzene ring) bending
700, 750	–CH <sub>3</sub> -CH <sub>2</sub> - (repetitive unit of cis-1,4-butadiene) bending
1150	S=O stretching, symmetrical C–H bond deformations in Si(CH <sub>3</sub> ) <sub>2</sub> and C = C–H (1,2 addition) bending vibrations.
1320, 1350	C-O stretching
1420	N–H (amide II) bending, C–H(–CH <sub>3</sub> -CH <sub>2</sub> -) bending, and –CH <sub>2</sub> deformations

### 3.2 PLS-DA

#### 3.2.1 Analysis of HMV and LMV tyre samples

The full range of Raman dataset of 400–2000  $\text{cm}^{-1}$  was subjected to PLS-DA using the mixOmics package in R software. Blue markers represented the HMV tyre samples, while orange markers represented the LMV tyre samples. Certain members of the dataset overlapped. The results of PLS-DA for class separation are presented in Fig. 2, where 95% confidence ellipses were drawn over each class. It may be noted that this representation involves only two latent variables (2D plot), however the overlap decreases when we consider an optimum (higher) number of latent variables based on the criteria mentioned earlier. Both the classes were mostly well separated, with minimal overlap of the classes.

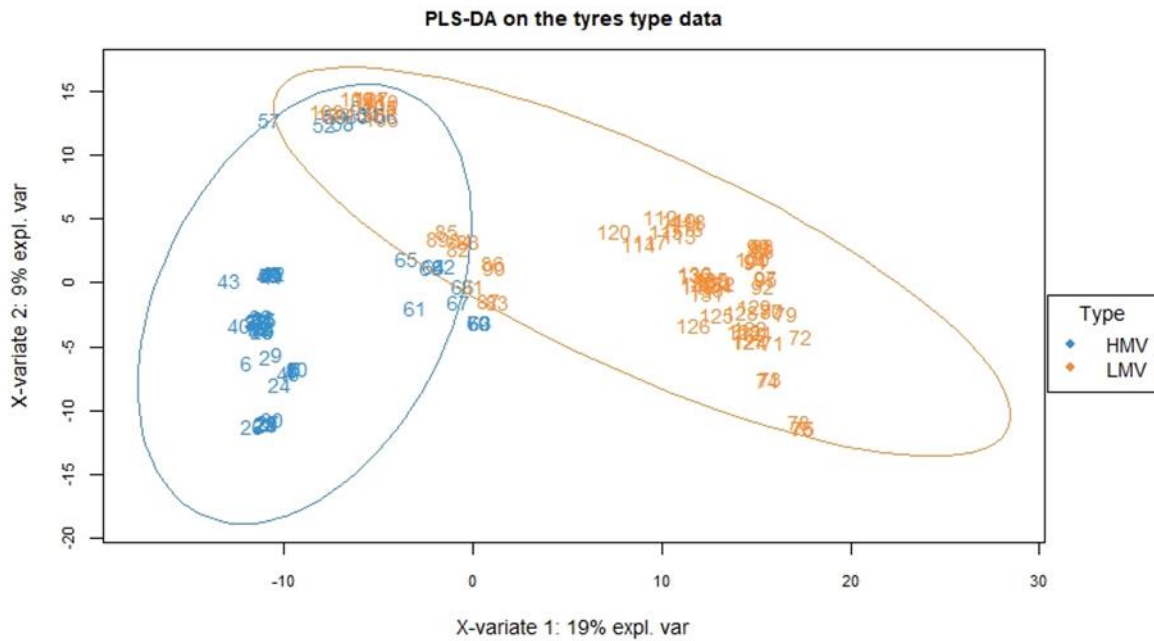


**Fig. 2: Two-dimensional (2D) PLS-DA plot.**

The performance of the model was evaluated based on the classification error rate (CER) by applying the “perf” function in the software. Samples were classified based on the optimum number of components through the repeated cross-validation method (five-fold at 10 repetitions). The lowest CER was determined by taking into account the optimum latent variables (LVs). As a key performance metric, CER determined how well the PLS-DA model differentiated these different classes. Referring to Fig. 3(a), the classification error rate with centroids distances varied between 10 to 15% and this figure was reasonably constant for 3 to 6 components. So, we can expect a classification error of 10 to 15 % between HMV and LMV tyres. The performance of the model was further evaluated from the ROC plot for 3 components and the area under the curve (AUC) figure was 0.9939, which is close to 1 (Fig. 3(b). The AUC figure never reached

the perfect level of 1 and was less than 0.999 even for higher number of latent variable. So, we only consider 3 latent variables. The BER was 0.14 and all the 21 HMV test samples were correctly predicted, but 6 of the 21 test LMV samples were incorrectly predicted as HMV.

USIM  
PREPRINT

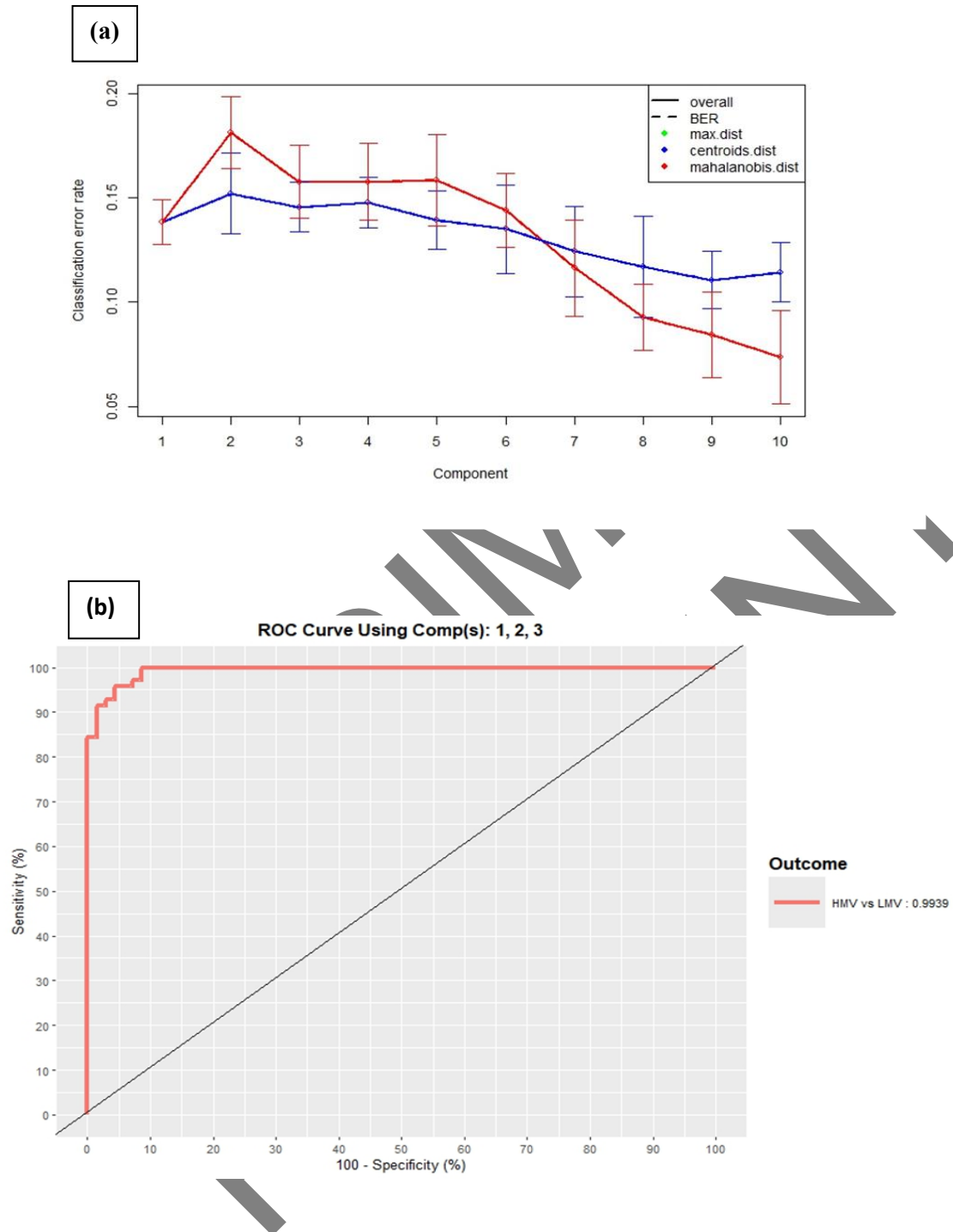


**Fig. 3: Classification error rates (CER) for two tyre types. (b) ROC for tyre samples (HMV versus LMV) on the third component.**

To assess the prediction ability of this model, 17 unknowns which were not part of the model were tested in the model and their type was predicted. Out of 9 LMV tyres 8 were correctly predicted to be so, however 1 was predicted as HMV type. All the 8 HMV tyres were predicted to be of this type only. Hence, we see a prediction error of 1 out of 17 around 6%. This might be due to the overlapping of some samples, having similar composition.

### 3.2.2 *Brand discrimination of tyre samples*

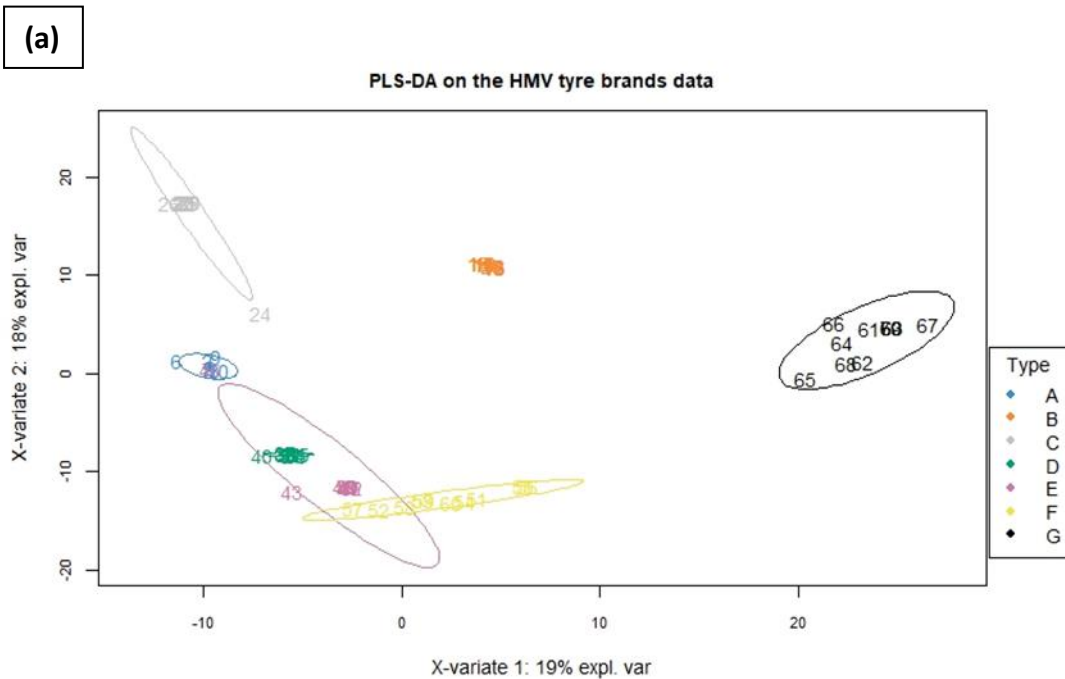
In the absence of vehicles involved in collision (e.g., hit-and-run incidents), rubber traces transferred from the tyres to the road produce skid marks that serve as evidence for forensic investigation. The results in the prior subsection addressed the question on the classification of tyre types. This subsection deals with the brand discrimination of tyre types.

Analysis of the dataset having 14 brands of both types of tyres i.e. LMV and HMV revealed possible overlap, as indicated by the two-dimensional plot in Fig. S.3, because of the large number of samples ( $n = 140$ , 10 samples for each brand) from Raman dataset. This overlap would have consequences in terms of misclassification of the brands. We have performed the analysis, but for the sake of brevity of the manuscript, the figures showing the analysis results have been provided in the supplementary material. Minimum classification error rate is obtained using the centroids distances and this error rate lies between 10-15 %. The classification error as evidenced from the ROC curves support this as the area under the curve (AUC) varies between 0.85 to 1 for these 14 brands and the balanced error rate turned out to be 0.12. The advantage of the PLS-DA method is that it is useful for multiclass classification unlike some other methods, but increasing number of classes impacts the classification accuracy. So, we thought it worth to

explore if the classification accuracy improves with considering the HMV and LMV tyres separately, given that we have already have a method of classification amongst the HMV and LMV types as detailed in the previous section.

### 3.2.3 Analysis of various tyre brands for HMV

There were seven different tyre brands for HMV tyre type in this study. Due to the small differences in these brands, the classification of tyre brands was very good with minimal overlapping of brands (Figure 4(a)). The results in Figure 4(b) revealed the separation of seven classes, with the constructed classification boundary at centroid distance. While the brands B, C, F and G are well separated from other brands and are having an AUC of 1, the AUC value for the remaining classes varies between 0.83 to 0.93. The classification error rate for the HMV brands is less than 10% (Fig S.4- Fig. S.5).



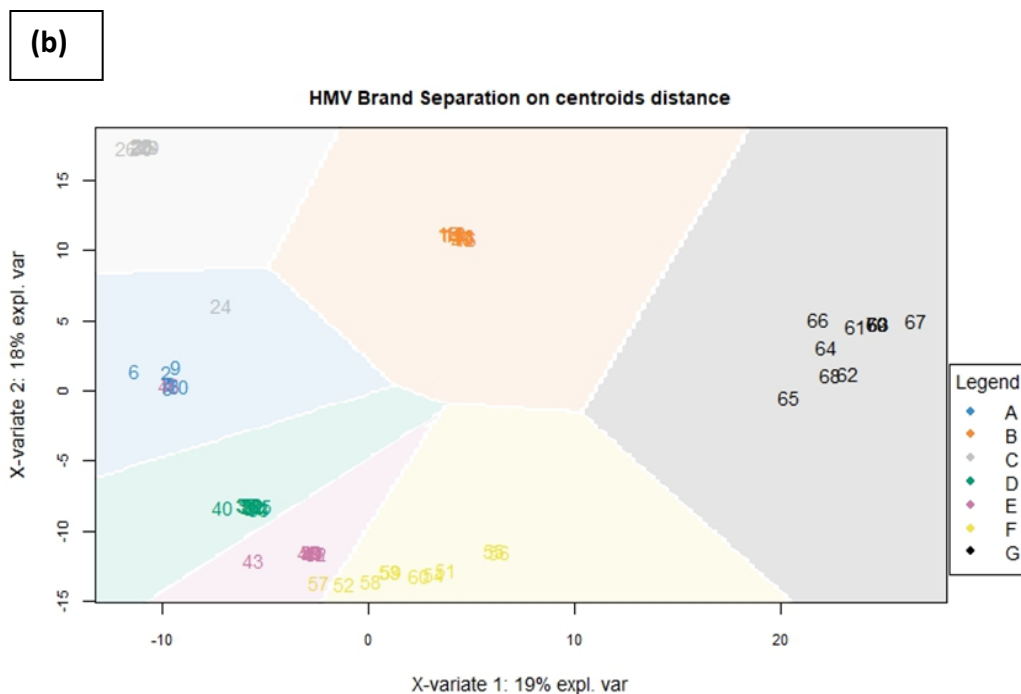


**Fig. 4: (a) 2D PLSDA of HMV tyre brands and (b) classification boundary in PLSDA for seven brands of HMV tyre type.**

### 3.2.4 Analysis of various tyre brands for LMV

Similarly, there were seven different tyre brands for LMV tyre type in this study. The classification of tyre brands showed overlapping of the M and N brands, as shown in Fig. S6 (a-b), depicting mostly well-separated samples by brands. Fig S.7-Fig S.8 shows that, for 3 components, the classification errors are generally less than those observed for the HMV samples films.

### 3.2.5 Real case scenario simulation

This study also explored real case scenario simulation, specifically in regards to tyre identification (after scratch of road). The real case simulation was carried out after 6 month completed the analysis of fresh tyre. The unknown tyres were collected and performed on dry track sunny day in Malaysia. Each test covered a different braking area. After three laps to heat up the tyres, the vehicle then braked from 40 km/h to 0 km/h under the employment of the same driver. Fig. S.9 shown the right tyre which 155/70 R12: Hankook Kinergy Eco 2 brand (Sample H) used for collection of unknown after scratch of road. Fig. S.10 show the yaw/skid marks deposited on the road carried out by Sample H from from 40 km/h to 0 km/. About 2–3 g of fresh tyre traces deposited on the road surface were collected and washed with acetone before these samples were properly sealed in plastic bags for further analysis. All samples were subjected to Raman spectroscopy and PLSDA to identify the origin of tyre traces. The results in Fig. 5 revealed that 10/12 of unknown samples after scratch of road as is evident overlap according to the brands. Here we see that 2 out of the 12 unknown samples were misclassified that amounts to an error of about 16.6 %. Despite the overlapping of brands for HMV and LMV tyre samples, the trained prediction model yielded correct identification by brands at the accuracy rate of 83.3%, as evidenced in Figure 5 and Table 4.

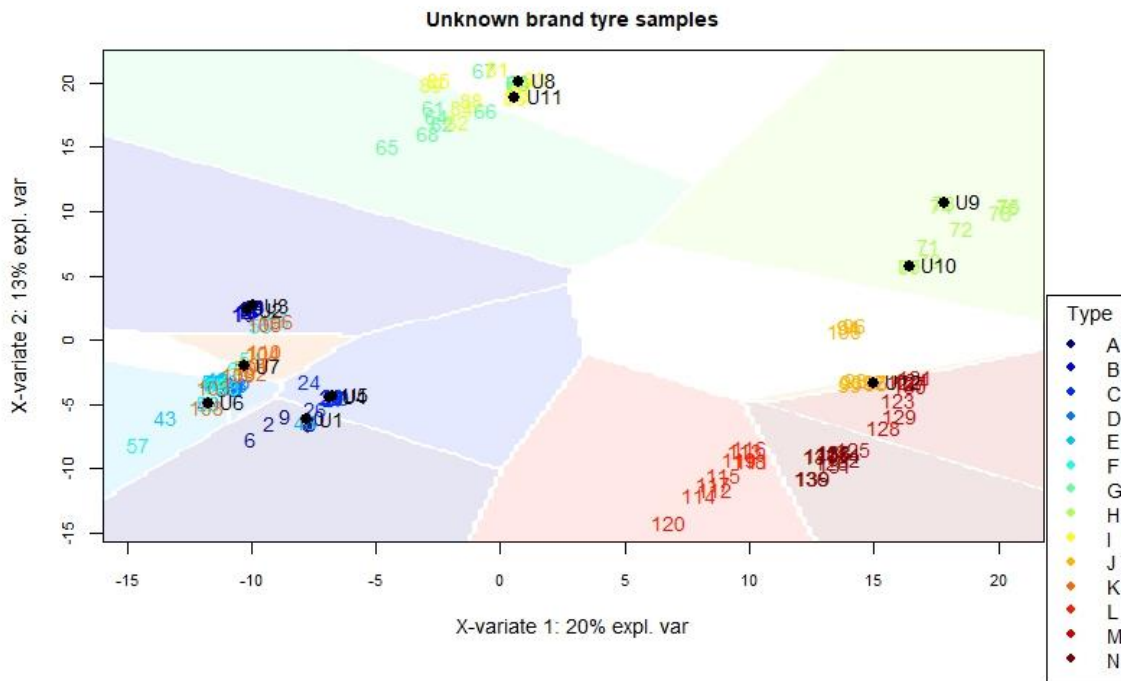


Fig. 5: Unknown sample prediction obtained from the road (unknown samples in black).

Table 4: Prediction of unknown samples obtained from the road on trained PLSDA model

Sample ID	Actual Class	Predicted Class	Prediction
U1	A	A	Correct
U2	B	B	Correct
U3	B	B	Correct
U4	C	C	Correct
U5	C	C	Correct
U6	D	D	Correct

U7	F	K	Incorrect
U8	G	I	Incorrect
U9	H	H	Correct
U10	H	H	Correct
U11	I	I	Correct
U12	J	J	Correct

### 3.2.6 Discussion critical review of work

Only a few studies analysed tyre (rubber) samples. A comprehensive review of related literature, including a recent study conducted by Kaur et al. [21], revealed that nearly 80% of studies on tyre analysis employed destructive techniques [1-3, 4,5-7,19,20], and the other 20% employed non-destructive techniques [13,14,21]. Since 1989, pyrolysis gas chromatography (Py-GC) has been commonly employed to analyse common rubber products [19], particularly for trace rubber residues. For instance, Sarkissian et al. [2,3] conducted two studies that utilised a destructive technique involving pyrolysis-gas chromatography mass spectrometry (Py-GCMS). These studies visually inspected the presence and absence of peaks and calculated the relative content percent (RCP) of butadiene, styrene, and isoprene in the tyre samples. However, only a sample (n = 12) was employed. These studies noted the application of chemometric techniques, specifically LDA, to discriminate tyres. Following Sarkissian et al.'s studies [2,3], Gueissaz [20] employed Py-GC combined with unsupervised PCA to analyse 10 tyre samples. The study reported accurate classification of all tyre trace samples through the clustering method and the correct assignment of all blind samples to the corresponding tyre sources. Following a decade after Gueissaz's [20] study, non-destructive analytical techniques have gained growing interest.

Two recent studies conducted by Haojun Du et al. [14] and Kaur et al. [21] focused on FTIR combined with chemometrics, which highlighted the application of ATR-FTIR combined with machine learning, specifically LR, RF, and WKNN. These studies explored the types of machine learning that yielded the best discrimination for tyre analysis. However, only Kaur's [21] study validated the application of machine learning through the utilisation of blind samples from three brands.

To date, there have been no studies that employed Raman spectroscopy with chemometrics. Addressing that, the current study utilised the PLS-DA modeling for real case scenario simulation. Unlike prior studies, this study's model yielded more reliable results for prediction in forensic case scenarios. Extending the study conducted by Kaur et al. [21], for the first time, alternative vibrational spectroscopy, specifically Raman spectroscopy, combined with chemometrics, was explored, yielding significant value in forensic investigations. Moreover, this study validated the applicability of the PLS-DA model in real case scenario simulation using unknown samples after scratch of road. Table 5 summarises the comparison of the present study with previous studies.

**Table 5: Comparison of the present study with previous studies**

No.	Instrumentation	Nature	Chemometrics	Findings	References
1	Pyrolysis-gas chromatography	Destructive	Not used	<ul style="list-style-type: none"> <li>Relative retention time (RRT) and relative content percent (RCP) obtained from rubber-soled shoes and their traces compared.</li> <li>No statistical test involved</li> </ul>	Jun-kai et al. (1989) [19]

No.	Instrumentation	Nature	Chemometrics	Findings	References
2	Pyrolysis-gas chromatography	Destructive	Not used	<ul style="list-style-type: none"> <li>Percentage of components (butadiene and styrene) was calculated.</li> <li>No statistical test involved</li> </ul>	Choi et al. (1999) [5]
3	Pyrolysis-gas chromatography	Destructive	Used	<ul style="list-style-type: none"> <li>42 rubber samples (from car) were analysed.</li> <li>The presence of components in chromatograms (styrene and limonene) was evaluated.</li> </ul>	Sarkissian, et al. (2004) [2]
4	Pyrolysis-gas chromatography	Destructive	Not used	<ul style="list-style-type: none"> <li>12 tyre samples were analysed using Py-GC.</li> <li>Tyre traces left on the road surface with sudden braking was identified from the original source.</li> <li>No statistical tests and chemometrics involved</li> </ul>	Sarkissian, et al. (2007) [3]
5	FTIR and Py-GC/MS	Non-destructive/ destructive	Used	<ul style="list-style-type: none"> <li>27 rubber samples (from car) were analysed.</li> <li>Accurate prediction rate of 94.9% by LDA based on brands only</li> </ul>	Lachowic et al. (2013) [4]
6	X-ray absorption near-edge	Non-destructive	Not used (t-test only)	<ul style="list-style-type: none"> <li>Analysis of the peak of height on tyres suggested</li> </ul>	Funatsuki et al. (2015) [1]

No.	Instrumentation	Nature	Chemometrics	Findings	References
	structure (XANES)			different sulphur chemical content among the tyre samples.	
7	ATR-FTIR	Non-destructive	Used (PCA and LDA)	<ul style="list-style-type: none"> <li>• 240 samples were analysed with FTIR analysis.</li> <li>• PCA and discriminant analysis were conducted for further analysis.</li> <li>• No prediction of unknown samples was applied.</li> <li>• No forensic case scenarios were discussed.</li> </ul>	He et al. (2019) [13]
8	ATR-FTIR	Non-destructive	Used	<ul style="list-style-type: none"> <li>• Comparison of different machine learning techniques</li> <li>• Prediction of unknown samples was applied.</li> </ul>	Kaur et al. (2024) [21]
9	Raman spectroscopy	Non-destructive	Used (PLSDA)	<ul style="list-style-type: none"> <li>• <b>Discrimination of 140 tyre samples (large samples).</b></li> <li>• <b>PLSDA for discrimination was performed.</b></li> <li>• <b>Prediction of unknown samples was applied.</b></li> </ul>	<b>Current study</b>

No.	Instrumentation	Nature	Chemometrics	Findings	References
				<ul style="list-style-type: none"> <li>• Further analysis on the unknown samples after scratch of road.</li> </ul>	

#### 4. Conclusions

This study served as the first to demonstrate a non-invasive, rapid, and reliable method for discrimination, specifically the combination of Raman spectroscopy and PLS-DA. The study recorded very good classification rate for both HMV and LMV samples. In forensic investigations, accurate identification of trace tyre source is pivotal. This study successfully demonstrated the application of chemometrics (PLSDA) to analytical technique (Raman spectroscopy) in crime scenes, pointing to the type and brand of the tyre and source. This study validated the suitability and applicability of the developed PLS-DA model for forensic case scenarios, as the model correctly predicted 83.3% of the unknown samples after scratch of road. As there have been no related studies, this study provided valuable insights that would greatly benefit forensic investigations involving the presence of tyre (rubber) samples in crime scenes. It is recommended for future research to explore the same non-invasive and rapid method using a larger sample, coupled with non-destructive techniques of ATR-FTIR, for crime scenes involving tyre (rubber) samples and also find the strength of association using the likelihood ratio approach.

#### References

1. A. Funatsuki, K. Shiota, M. Takaoka, Y. Tamenori, Forensic analysis of tyre rubbers based on their sulfur chemical states, *Forensic Sci. Int.* 250 (2015) 53–56, <https://doi.org/10.1016/j.forsciint.2015.02.022>.
2. G. Sarkissian, J. Keegan, E. Du Pasquier, J.-P. Depriester, P. Rousselot, The analysis of; tyres and tyre traces using FTIR and Py-GC/MS, *Can. Soc. Fore. Sci. J.* 37 (2004) 19–37.
3. G. Sarkissian, The analysis of tyre rubber traces collected after braking incidents using pyrolysis-gas chromatography/mass spectrometry, *J. Forensic Sci.* 52 (2007) 1050–1056.
4. T. Lachowicz, J. Zięba-Palus, P. Ko' scielniak, Chromatographic analysis of tyre rubber samples as the basis of their differentiation and classification for forensic purposes, *Anal. Lett.* 46 (2013) 2332–2344.
5. S.-S. Choi, Characterization of bound rubber of filled styrene-butadiene rubber compounds using pyrolysis-gas chromatography, *J. Anal. Appl. Pyrol.* 55 (2000)161–170.
6. K.S. Kapgate, R.V. Phadke, S.S. Apte, V.J. Thakre, S.V. Ghumatkar, Characterization of rubber tyre using simultaneous thermal analysis and microXRF: A comparative study in forensic investigation, *Chem. Sci. Trans.* 11 (2022) 7–14.
7. J. Lucchi, D. Gluck, S. Rials, L. Tang, M. Baudelet, Tyre classification by elemental signatures using laser-induced breakdown spectroscopy, *Appl. Spectrosc.* 75 (2021) 747–752.
8. R. Chauhan, R. Kumar, V. Sharma, Soil forensics: a spectroscopic examination of trace evidence, *Microchem. J.* 139 (2018) 74–84.
9. V. Sharma, S. Bhardwaj, R. Kumar, On the spectroscopic investigation of Kohl stains via ATR-FTIR and multivariate analysis: Application in forensic trace evidence, *Vib. Spectrosc.* 101 (2019) 81–91, <https://doi.org/10.1016/j.vibspec.2019.02.006>.
10. P. Pienpinijtham, C. Thammacharoen, S. Naranitad, S. Ekgasit, Analysis of cosmetic residues on a single human hair by ATR FT-IR microspectroscopy, *Spectrochim. Acta A Mol. Biomol. Spectrosc.* 197 (2018) 230–236.

11. A. Sharma, V. Sharma, Forensic analysis of cigarette ash using ATR-FTIR spectroscopy and chemometric methods, *Microchem. J.* 178 (2022), 107406, <https://doi.org/10.1016/j.microc.2022.107406>.
12. R. Kumar, K. Sharma, V. Sharma, Bloodstain age estimation through infrared spectroscopy and Chemometric models, *Sci. Justice* 60 (2020) 538–546.
13. X. He, J. Wang, Rapid and nondestructive forensic identification of tyre particles by attenuated total reflectance – fourier transform infrared spectroscopy and chemometrics, *Anal. Lett.* 53 (2019) 714–734.
14. H. Du, Forensic characterization of tyres by attenuated total reflectance-Fourier transform infrared (ATR-FTIR) spectroscopy and machine learning algorithms, *Anal. Lett.* (2022) 1–15.
15. M.N.M. Asri, R. Verma, N.A.M. Nor, M. H. Ibrahim, V. Sharma, Rapid non-destructive techniques to identify the traces of Kajal using chemometrics; A comparison of ATR-FTIR and Raman spectroscopy, *Microchemical J.* 169, (2021), <https://doi.org/10.1016/j.microc.2021.106556>.
16. A. Sharma, R. Chauhan, R. Kumar, P. Mankotia, R. Verma, V. Sharma, A rapid and non-destructive ATR-FTIR spectroscopy method supported by chemometrics for discriminating between facial creams and the classification into herbal and non-herbal brands, *Spectrochim. Acta Part A Mol. Biomol. Spectrosc.* 258 (2021), <https://doi.org/10.1016/j.saa.2021.119803> 119803
17. M.N.M. Asri, N.F. Nestrgan, N.A.M. Nor, R. Verma, On the discrimination of inkjet, laser and photocopier printed documents using Raman spectroscopy and chemometrics: application in forensic science, *Microchem. J.* 165 (2021) 106136. <https://doi.org/10.1016/j.microc.2021.106136>.
18. T. Arora, R. Verma, R. Kumar, R. Chauhan, B. Kumar, V. Sharma, Chemometrics based ATR-FTIR spectroscopy method for rapid and non-destructive discrimination between eyeliner and mascara traces, *Microchem. J.* 164 (2021), <https://doi.org/10.1016/j.microc.2021.106080> 106080.

19. D. Jun-kai, L. Hai-shan, A study of identification of trace rubber residues in marks from rubber-soled shoes and tyres by Py-GC, *Forensic Sci. Int.* 43 (1989) 45–50, [https://doi.org/10.1016/0379-0738\(89\)90121-7](https://doi.org/10.1016/0379-0738(89)90121-7).
20. L. Gueissaz, G. Massonnet, Tyre traces – discrimination and classification of pyrolysis-GC/MS profiles, *Forensic Sci. Int.* 230 (2013) 46–57, <https://doi.org/10.1016/j.forsciint.2012.10.013>.
21. N. Kaur, A. Sharma, V. Sharma, Advancing automobile identification and brand discrimination from tyre rubber through Machine learning algorithms for forensic investigations, *Spectrochimica Acta Part A: Molecular and Biomolecular Spectroscopy*, 09, 2024, 123821, 1386-1425, <https://doi.org/10.1016/j.saa.2023.123821>.
22. G. Socrates, J. Wiley, *Infrared and Raman characteristic group frequencies: tables and charts*, John Wiley & Sons Ltd., 2015.